Zeitschrift: Bulletin der Vereinigung Schweiz. Petroleum-Geologen und -Ingenieure
Band: 39 (1972-1973)
Heft: 96

Artikel: Some modern techniques in hydrogeology
Autor: Haefeli, Charles
DOI: https://doi.org/10.5169/seals-198504

Bull. Ver. Schweiz. Petrol.-Geol. u. -Ing., Vol. 39, Nr. 96, Mai 1973, S. 51–68

Some modern techniques in hydrogeology

with 15 figures

by CHARLES HAEFELI*)

Table of contents

1. Aquifer evaluation by computer

1.1. Introduction

The dynamics of groundwater flow systems under natural conditions are extremely complicated, and in any case very difficult to analyse. Consequently many attempts have been made to master them as closely as possible. However, due to the inherent complexity of geological conditions – anisotropy, non-homogenity, stratification – all mathematical solutions developed for this purpose are in fact strictly valid only for idealized conditions.

In the field of well hydraulics, new methods are continuously being presented to handle varying geological cases by more realistic approaches. However, on a regional scale the situation is far more complicated, and the simplifications have to be carried further to deal with ever-changing geological conditions and to account for environmental factors affecting groundwater flow. Obviously, certain limits exist to any meaningful simplification, but the assumed mathematical model shall still reflect reality to an acceptable degree. On the other hand the sophistication of the model should remain within the limits of the accurracy and availability of the basic input parameters.

Depending on the available data and time, and on the kind of final results required, the optimum procedures for the analysis of regional groundwater flow systems have to be determined. In most cases several methods should be used to reach the objective in

*) Electro-Watt Engineering Services Ltd., Zurich.

different ways, the most decisive and versatile of which are often modern simulation models. On the following pages certain digital simulation techniques for the analysis of regional groundwater problems are briefly introduced. The models have been taken over from the field of research hydrogeology, adapted to practical conditions and in part further developed.

1.2. *Freeze-Witherspoon model* (Figures 1 and 2)

Description

This model simulates steady-state regional groundwater flow patterns in a three-dimensional, non-homogeneous, anisotropic groundwater basin. It is based on RICHARDS equation (1) which has been developed from Darcy's law and the steady-state equation of continuity. The partial differential equations, which are solved by finite difference approximations and the successive over relaxation technique, yield the distribution of the fluid potential.

$$\frac{\delta}{\delta x}\left[K(x,y,z)\frac{\delta \varnothing}{\delta x}\right]+\frac{\delta}{\delta y}\left[K(x,y,z)\frac{\delta \varnothing}{\delta y}\right]+\frac{\delta}{\delta z}\left[K(x,y,z)\frac{\delta \varnothing}{\delta z}\right]=0$$

or in two dimensions:

$$\frac{\delta}{\delta x}\left[K(x,z)\frac{\delta \varnothing}{\delta x}\right]+\frac{\delta}{\delta z}\left[K(x,z)\frac{\delta \varnothing}{\delta z}\right]=0 \quad (1)$$

where:

K = permeability coefficient
$\varnothing$ = hydraulic head

In order to determine the regional groundwater flow pattern it is necessary to know:
1) the dimension of the basin
2) the water table configuration
3) the permeability distribution from the sub-surface stratigraphy

The computer output is in the form of printed values of the hydraulic head and of plotted equipotential nets in vertical cross-sections through the basin. Depending on the available computer facilities and the required accuracy the grid network may contain well over 1000 nodes (approx. 26000 nodes for the UNIVAC 1107).

Application

a) Initial basin yield

The potential pattern determined by the mathematical model and confirmed by field measurements can be used to construct basinwide quantitative flow nets. Using a series of flow nets, which are orientated perpenticularly to the main flow direction, the groundwater runoff, the quantity of recharge and discharge, may be computed at any point over the entire basin, or at any desired cross-section. Thus, the initial basin or sub-basin yield, corresponding in some cases with the safe yield, may be calculated.

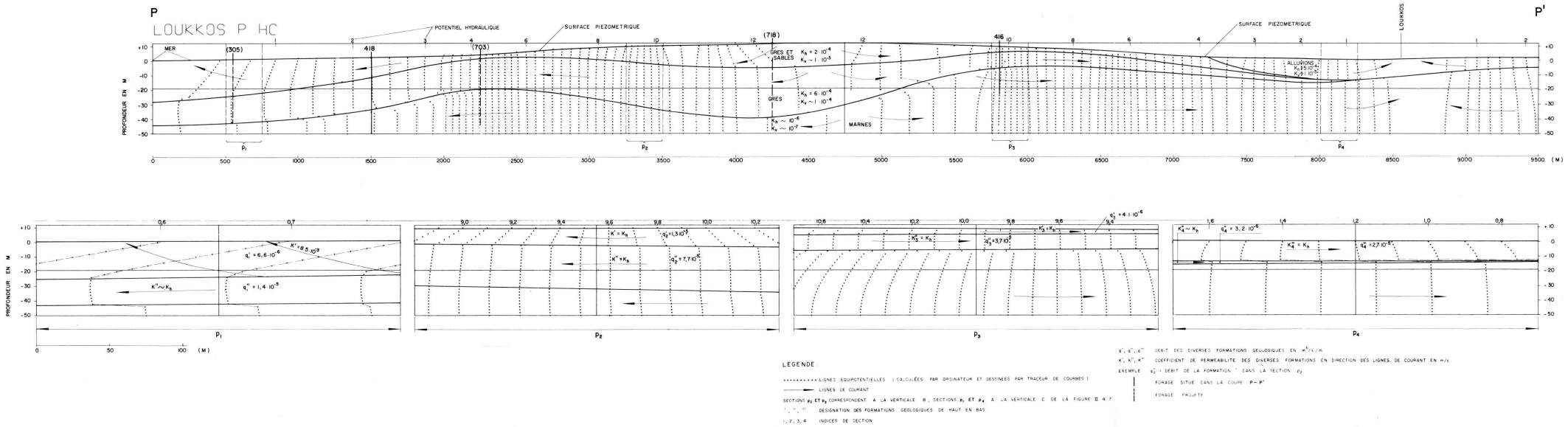

Fig. 1: Hydrogeological cross section through Loukkos aquifer (Morocco), analysis of groundwater runoff (recharge and discharge) (computer plot).

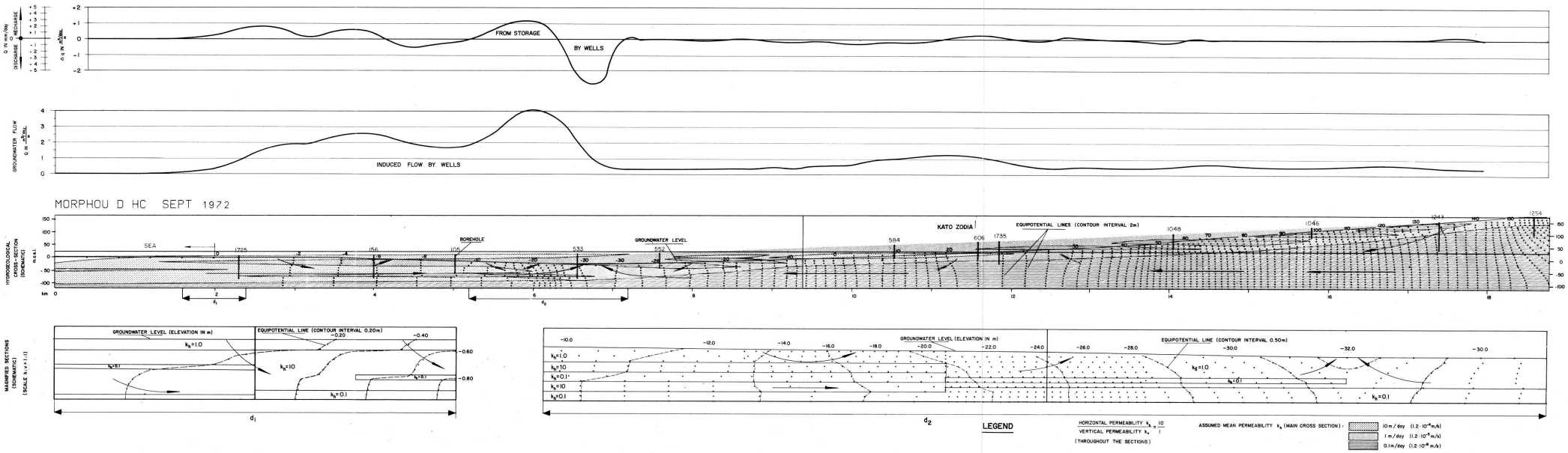

Fig. 2: Hydrogeological cross section through Morphou aquifer (Cyprus), analysis of groundwater runoff (recharge and discharge) and sea water intrusion (partly computer plot).

b) Effect of future groundwater withdrawals or artificial recharge

Also the mathematical model analyses steady-state conditions, any change in the basin with regard to discharge and recharge can be easily simulated by means of the «inverse method». The groundwater flow system is analyzed for any desirable, permissable or extreme water level configuration. By this means the quantity of the concerning withdrawals or artificial recharges concerned can be computed, and the management of the groundwater resources may be determined accordingly. In this sense the model becomes transient.

c) Water balance

The relation between surface- and groundwater-runoff, as well as the extend of groundwater evaporation and surface water infiltration, are visible from the model. In short, it can be stated that the nature of the groundwater flow pattern reflects the effect of the components of the hydrologic cycle, which are made evident in quantity and areal concentration by the model.

1.3. Pinder model (Figures 3 and 4)

Description

This programme simulates the response of a confined aquifer to pumping from wells at a constant rate for any given length of time, to recharge from various sources (wells, rivers, lakes), and to the infiltration of rainfall. The groundwater reservoir may be irregular in shape and non-homogeneous. The model is based on the following equations (2):

$$\frac{\delta}{\delta x_i}\left(T_{ij}\frac{\delta h}{\delta x_j}\right) = S\frac{\delta h}{\delta t} + W(x, y, t) \quad (2)$$

where:

T_{ij} = transmissitivity tensor
h = hydraulic head
S = storage coefficient (dimensionless)
t = time
W = volume flux per unit area

The partial differential equations are solved in a similar way to those of the previous model.

The following main basic hydro-geological inputs are required:

- Transmissibility
- Storage coefficient
- Location and rate of extraction sources
- Location and hydraulic conductivity of stream and lake beds
- Vertical leakage from precipitation (if any)
- Time

The computer output is in the form of a list showing the exact change of head (draw down) at each node, and as a plan view plot showing an alphanumerical array for a quick overview. Contour lines of the depression areas may be constructed accordingly.

The density of the grid network (array) can be chosen according to the size of the area, the available data, the required accuracy and the computer facilities (maximum number of nodes for the Univac 1107 approx. 8000).

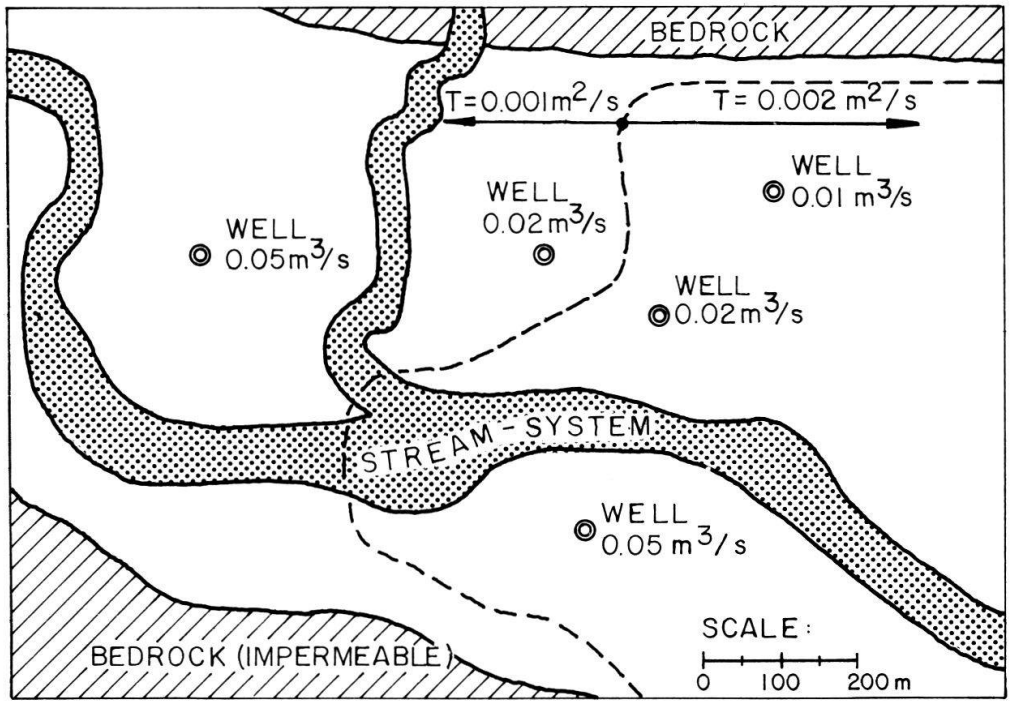

Fig. 3: a) sketch of a well field under confined conditions (pumping rate of wells, Q, in m^3/s; transmissibility, T; storage coefficient, $S = 3.5 \cdot 10^{-3}$; mean streambed thickness, $m = 3$ m; mean streambed permeability, $K = 1.5 \cdot 10^{-4}$ m/s; no infiltration from rainfall).

```
R 1 1 1 1 1 1 1
R R 1 1 1 1 1 1 1 1 R 1 1 1 1 1 1 1 1 1 1 1 1 1
0 R 1 1 1 1 1 1 1 R R 1 1 1 1 1 1 1 1 1 1 1 1 1
0 R 1 2 2 2 1 1 1 R 1 1 1 1 1 1 1 1 2 2 2 1 1 1 1
0 R 2 3 4 4 2 1 1 R 1 1 1 1 1 1 1 2 2 2 W 2 1 1 1 1
R R 3 6 9 6 4 2 1 R 1 1 2 3 2 2 2 2 2 2 2 1 1 1 1
R 2 4 9 W 9 5 2 1 R 1 1 2 W 3 2 2 2 2 2 1 1 1 1 1
R 1 3 6 9 6 4 2 1 R 1 1 2 3 3 3 3 3 2 2 1 1 1 1 1
R R 2 3 4 4 2 1 R R 1 1 1 2 2 3 W 3 2 1 1 1 1 1 1
0 R R 2 2 2 1 1 R 1 1 1 1 1 2 2 3 2 2 1 1 1 1 1 1
0 R R 1 1 1 1 1 R R 1 1 1 1 1 1 2 2 1 1 1 1 1 1 1
0 R R R 1 1 1 1 1 R R R R R R R 1 1 1 1 1 1 1 1 1
0 0 R R R R R R R R R R R R R R R R R R 1 1 1 1 1
0 0 0 R R R R R R R R R 1 2 3 2 2 1 R R R 1 1 1 1
0 0 0 0 0 0 0 1 R R R 1 2 4 6 4 3 2 1 R R 0 0 0 1
0 0 0 0 0 0 1 1 1 1 1 2 3 6 W 6 3 2 1 1 R R 0 0 1
  0 0 0 0 1 1 1 1 1 1 1 2 3 4 6 4 3 2 1 1 1 R R 0 0
    0 0 0 1 1 1 1 1 1 1 2 2 3 4 3 2 2 1 1 1 R R 0 0
      0 0 1 1 1 1 1 1 1 1 2 2 2 2 2 1 1 1 1 1 R R 0
                  1 1 1 1 1 1 1 1 1 1 1 1 1 1 R R
```

b) numeric contours of the same well field showing the depression of the piezometric surface in meters after 9 hours of continuous pumping (R = stream system, W = well, 1 .... 9 = drawdown in meters) (computer plot).

ITERATION NUMBER 60
SIZE OF TIME STEP IN SECONDS= .526+04
DURATION OF PUMPING AT THIS PRINTOUT IN SECONDS= 32468.511
MINUTES= 541.142
HOURS= 9.019
DAYS= .376

QUANTITY PUMPED ACCORDING TO CONE OF DEPRESSIONIN CUBIC m = 3547.5551000

QUANTITY PUMPED ACCORDING TO WELL DISCHARGE IN CUBIC m = 4545.591500

ESTIMATE FROM PUMPING LESS ESTIMATE FROM DRAWDOWN = 998.036500

DIFFERENCE AS A PERCENT OF VOLUME PUMPED= 21.956141

DRAWDOWN IN METER(1) DRAWDOWN IN METER(2)

1	.0	.0	.0	.0	.0	.0	.0	.0	.0	.0	.0	.0	.0	.0	.0	.0	.0	.0	.0	.0	.0	.0	.0	.0	.0	.0	.0	.0
2	.0	.0	.0	.0	.0	.0	.0	.0	.0	.0	.0	.0	.0	.0	.0	.0	.0	.0	.0	.0	.0	.0	.0	.0	.0	.0	.0	.0
3	.0	.0	.0	.1	.1	.2	.2	.1	.0	.0	.0	.0	.0	.0	.0	.0	.0	.0	.0	.0	.0	.0	.0	.0	.0	.0	.0	.0
4	.0	.0	.0	.2	.3	.3	.3	.2	.1	.1	.0	.0	.1	.1	.2	.2	.4	.5	.6	.6	.7	.6	.4	.3	.2	.2	.0	
5	.0	.0	.0	.3	.6	.8	.7	.5	.3	.1	.0	.0	.1	.2	.3	.4	.5	.6	.7	.8	.9	.7	.5	.4	.2	.2	.0	
6	.0	.0	.0	.8	1.4	1.8	1.5	1.0	.5	.2	.0	.1	.2	.4	.5	.6	.7	.8	.9	1.1	1.4	1.0	.7	.4	.3	.2	.0	
7	.0	.0	.0	1.5	3.0	4.0	3.1	1.9	1.0	.4	.0	.2	.4	.7	1.0	1.0	1.0	1.1	1.2	1.6	(2.7)	1.4	.8	.5	.3	.2	.0	
8	.0	.0	.0	2.6	5.6	8.9	5.8	3.1	1.5	.6	.0	.3	.7	1.3	2.0	1.6	1.5	1.4	1.4	1.5	1.6	1.1	.7	.4	.3	.2	.0	
9	.0	.0	1.1	3.7	8.8	(21.1)	8.9	4.0	1.8	.6	.0	.3	.9	2.0	(4.6)	2.5	2.0	2.0	1.7	1.4	1.2	.9	.6	.4	.3	.2	.0	
10	.0	.0	.9	2.7	5.6	8.9	5.8	3.1	1.4	.5	.0	.3	.7	1.4	2.3	2.2	2.5	2.9	2.1	1.5	1.1	.7	.5	.3	.2	.2	.0	
11	.0	.0	.0	1.3	2.9	4.0	3.1	1.9	.9	.0	.0	.2	.5	.9	1.4	1.9	2.9	(5.2)	2.6	1.5	1.0	.6	.4	.3	.2	.2	.0	
12	.0	.0	.0	.0	1.2	1.7	1.5	1.0	.5	.0	.0	.1	.3	.5	.8	1.3	1.8	2.5	1.8	1.2	.8	.5	.3	.2	.1	.1	.0	
13	.0	.0	.0	.0	.4	.7	.6	.4	.2	.0	.0	.1	.1	.2	.4	.6	.9	1.2	1.0	.7	.5	.3	.2	.1	.1	.1	.0	
14	.0	.0	.0	.0	.0	.2	.2	.2	.1	.0	.0	.0	.0	.0	.0	.0	.0	.4	.4	.4	.2	.2	.1	.1	.1	.1	.0	
15	.0	.0	.0	.0	.0	.0	.0	.0	.0	.0	.0	.0	.0	.0	.0	.0	.0	.0	.0	.0	.0	.1	.1	.0	.0	.0	.0	
16	.0	.0	.0	.0	.0	.0	.0	.0	.0	.0	.0	.0	.0	.9	1.6	2.1	1.7	1.1	.6	.0	.0	.0	.0	.0	.0	.0	.0	
17	.0	.0	.0	.0	.0	.0	.0	.0	.0	.0	.0	.0	.8	2.0	3.5	5.2	3.6	2.2	1.2	.5	.0	.0	.0	.0	.0	.0	.0	
18	.0	.0	.0	.0	.0	.0	.0	.0	.1	.2	.3	.6	1.4	2.8	5.4	(11.6)	5.5	2.9	1.5	.7	.3	.0	.0	.0	.0	.0	.0	
19	.0	.0	.0	.0	.0	.0	.0	.0	.1	.2	.4	.7	1.4	2.4	3.9	5.6	4.0	2.5	1.4	.8	.4	.1	.0	.0	.0	.0	.0	
20	.0	.0	.0	.0	.0	.0	.0	.0	.1	.2	.4	.7	1.1	1.8	2.5	3.0	2.5	1.8	1.1	.6	.3	.1	.0	.0	.0	.0	.0	
21	.0	.0	.0	.0	.0	.0	.0	.0	.1	.2	.3	.5	.8	1.1	1.5	1.6	1.4	1.1	.7	.4	.2	.1	.0	.0	.0	.0	.0	
22	.0	.0	.0	.0	.0	.0	.0	.0	.0	.0	.3	.4	.5	.6	.7	.7	.7	.5	.4	.2	.1	.1	.0	.0	.0	.0	.0	
23	.0	.0	.0	.0	.0	.0	.0	.0	.0	.0	.0	.0	.0	.0	.0	.0	.0	.0	.0	.0	.0	.0	.0	.0	.0	.0	.0	

Fig. 4: Numeric planview plot of the same well field (Figure 3) showing the exact drawdown at each node after 9 hours of continuous pumping (Circles = location of wells; difference as a percent of volume pumped = amount of infiltration from stream system) (computer plot).

Application

Since it represents a true transient model, the effect of extraction, recharge and infiltration on the piezometric surface may be computed for any length of time (minutes, hours, ...). Its wide field of application might be enumerated as follows:

a) Planning of the development of new groundwater resources.
b) Optimization of extraction in existing well fields.
c) Evaluation of boundary condition effects on production wells.
d) Management of groundwater resources (permissable withdrawal, forecast of long-term effects, areal redistribution of extraction).

For the time being the model runs strictly for confined conditions. However, considerable efforts are being made to adjust an alternative version for phreatic conditions.

1.4. *Californian model* (Figure 5)

Description

After processing all groundwater balance parameters this model generates groundwater level fluctuations reflecting the change of the input variables. Its principle is comparable to the parametric synthesizing of stream hydrographs. It works for confined and unconfined conditions. Its fundamental mathematic expression (3) is again based on Darcy's law and the equation of continuity, and can be written as follows:

$$\Sigma_i \left[(h_i = h_B) \frac{T_{i,B} W_{i,B}}{L_{i,B}} \right] + A_B Q_B = A_B S_B \frac{dh_B}{dt} \qquad (3)$$

where:

h_B = representative groundwater level (head) of the general unit area B.
h_i = representative groundwater level of a unit area adjacent to area B.
$L_{i,B}$ = distance between the nodal points of areas B and i.
$T_{i,B}$ = representative transmissibility between areas B and i.
$W_{i,B}$ = width through which the subsurface flow occurs between areas B and i.
A_B = area of general unit area B.
Q_B = rate of net surface inflow and outflow of general unit area B.
S_B = representative specific yield of sediments in general area B.
t = time.

A horizontal nodal network consisting either of polygons or squares is spread over the study area. The number of the nodes is rather limited more by the preparatory work on the large amount of necessary input data then by the computer capacity. The output of the computer is a groundwater hydrograph for every single node and a rough alphanumerical planview plot. The following main input parameters are required:

- Permeability
- Hydraulic conductivity
- Specific yield (storage coefficient)
- Infiltration rate (from streams, rainfall, irrigation)
- Groundwater evapotranspiration
- Consumptive use (extraction)
- Initial hydraulic gradient

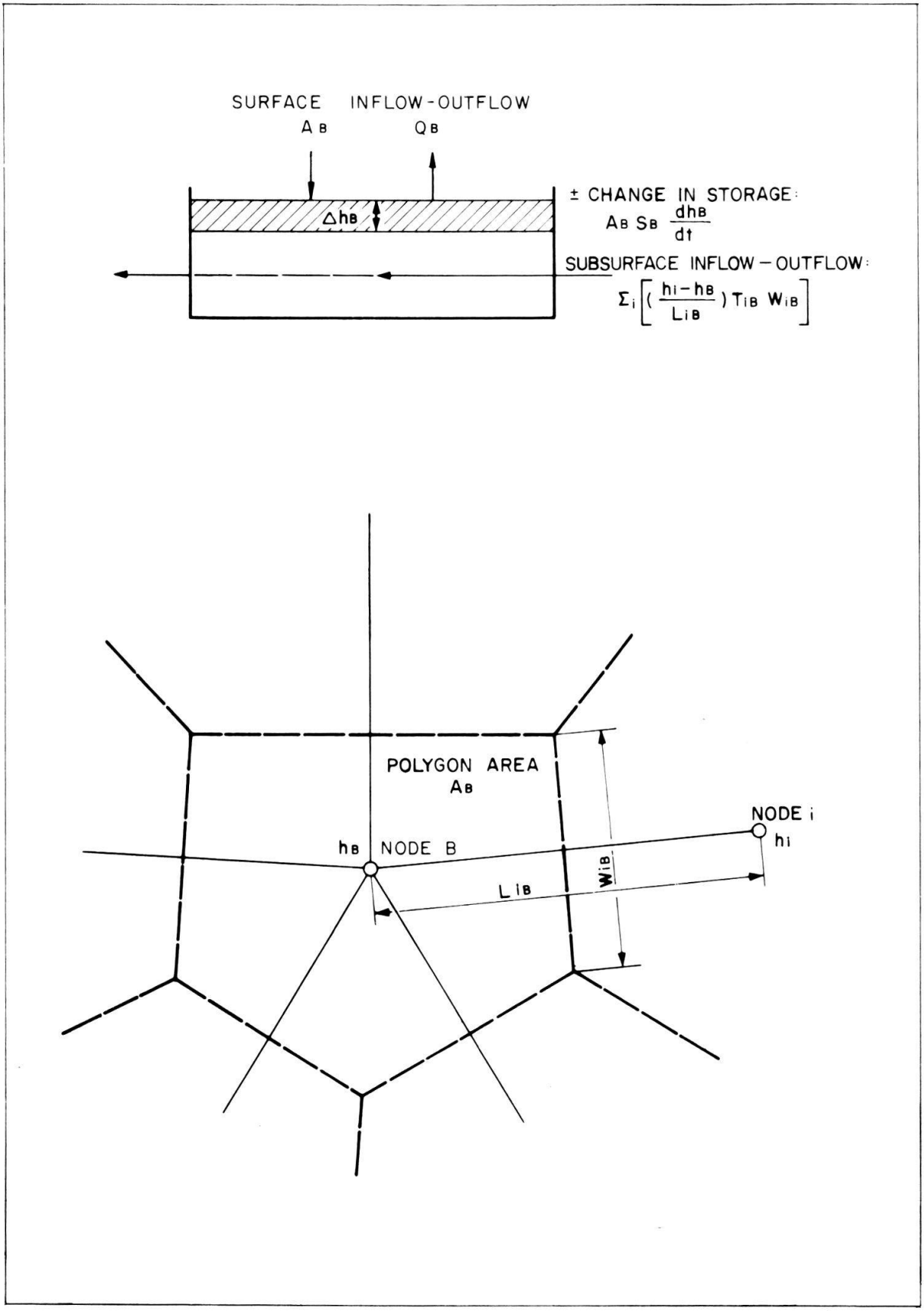

Fig. 5: Schematic sketch of generalized groundwater flow equation of Californian model (above: cross-section of node B, below: planview of node B).

Application

The model computes a complete groundwater balance for any type of aquifer, provided that all input data are available and prepared carefully beforehand. The fluctuation of the groundwater level reflects the effect of any recharge or discharge. The model is well suited to analyse the present and future management of groundwater resources, and can in fact be qualified as a very comprehensive regional groundwater flow model. However, under some circumstances it exhibits a certain clumsiness (§ 1.6).

1.5. Auxiliary models for statistical analyses (Figures 6 and 7)

In many cases a large quantity of data and records is available which has to be digitized, evaluated or reduced to reliable figures, before it can be used as straight computer input material. Statistical analyses are often required for this purpose.

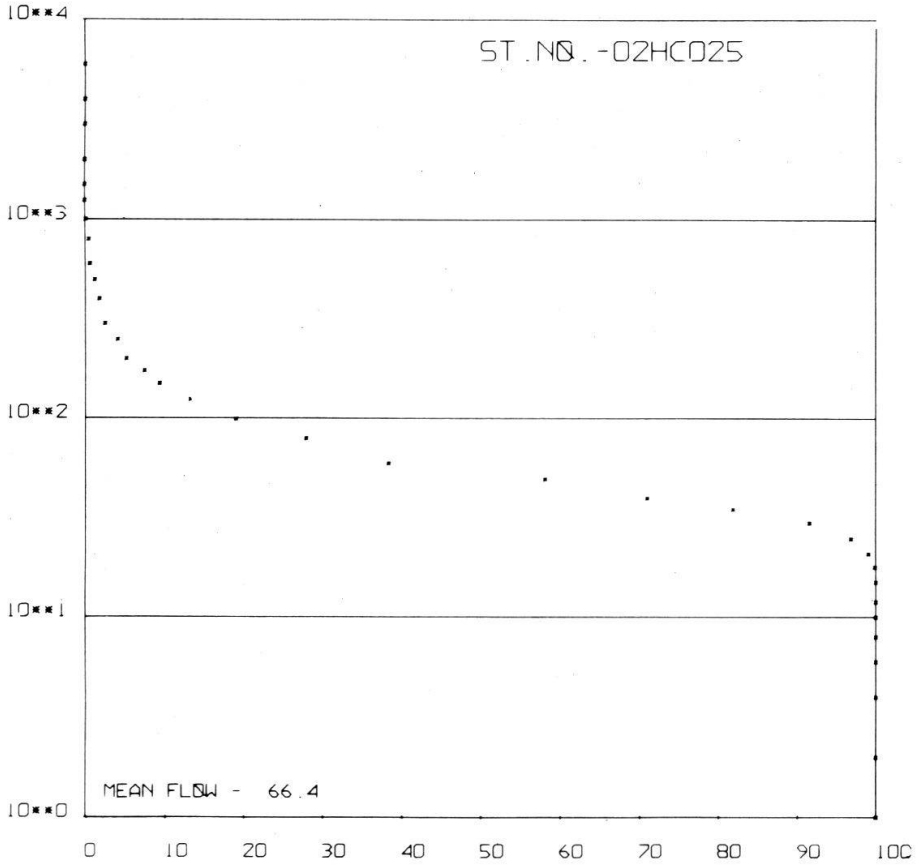

Fig. 6: Runoff frequency computer plot of gauging station 02HC025.

Model Freq

The statistical distribution of hydrological and hydrogeological data is in most cases, as in other working fields, skewed to the right, i.e. the medium is smaller than the mean. Thus, to avoid substantial errors, the medium should be used as input rather than the mean. This procedure should be applied whenever the available data shows a strong variation due to measuring or estimating errors, e.g. extraction data of farmer wells. Another example is the base flow analysis of rivers, where the discharge of a

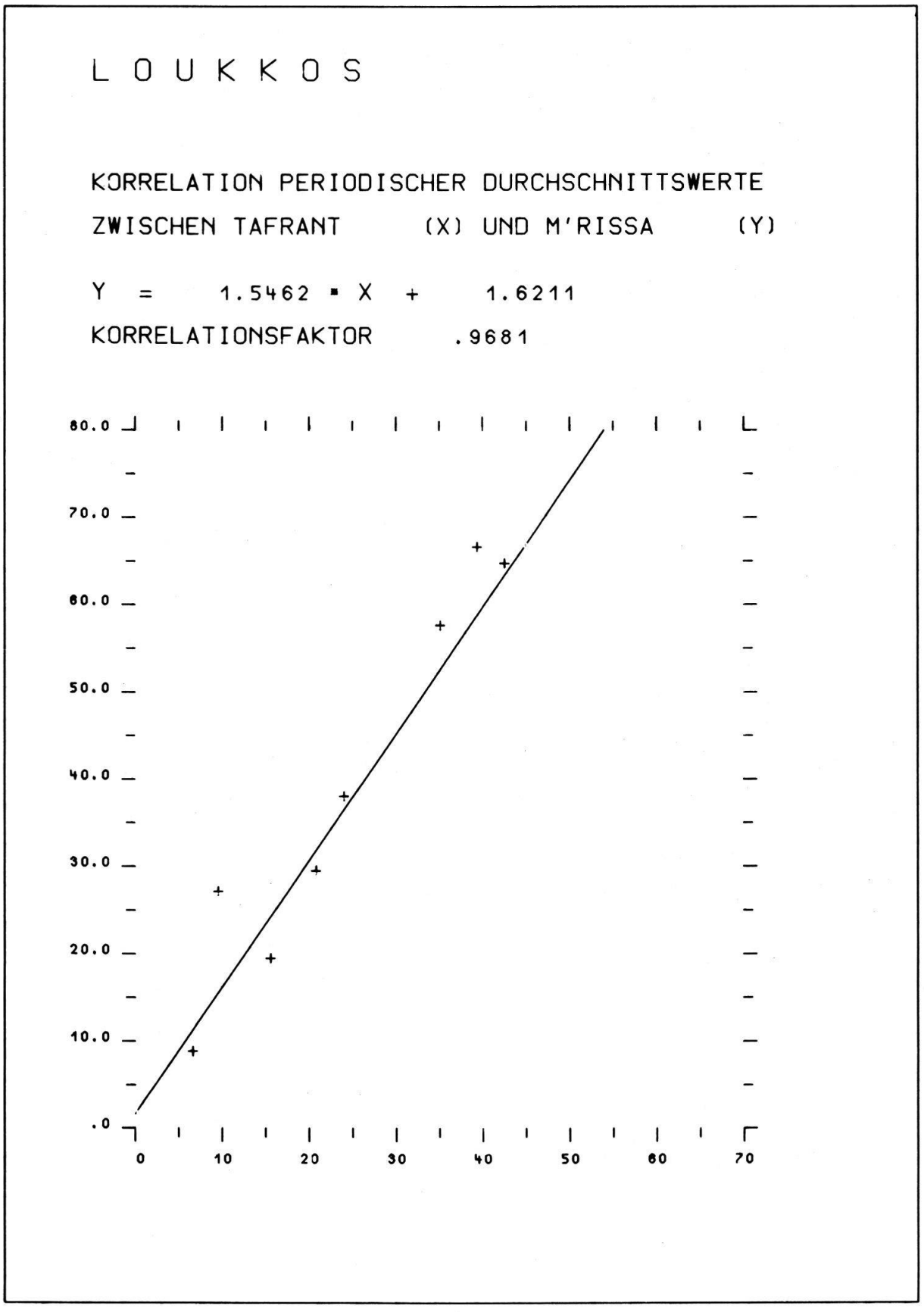

Fig. 7: Correlation between the gauging stations Tafrant and M'Rissa (computer plot).

stream equalled or exceeded during 90% of time is in many cases a very useful parameter to characterize the groundwater inflow. To avoid elaborate computations the frequency program FREQ is introduced for these statistical evaluations, producing a frequency distribution plot.

Model LINKOR

This model is handy whenever different sets of data have to be brought into correlation with each other, for example the correlation of streamflows or of groundwater flow components. Its output is printed and plotted, showing the best fit line, the corresponding regression function as well as the correlation factor.

1.6. Limitations of the computer models

By making use of the computer techniques which have been described, the solution of almost any meaningful regional groundwater problem is considerably eased. Their application is however rather limited by the availability and accuracy of the input data, as has previously been mentioned, shortcomings, however, which equally impair classic evaluation methods. The more detailed the required inputs for the model are, the more affected it is by the lack of data. The California model for example provides a most comprehensive groundwater balance which can be envisaged by many hydrogeological studies. But if the required input parameters do not attain a certain level of accuracy, their large number might seriously aggravate the calibration of the model. In such cases it is advisable to use a less comprehensive model, as for example that of Freeze-Witherspoon, matching facilities to the data and reaching the groundwater balance by a detour. Whoever has attempted to estimate infiltration rates and storage coefficients will be very cautious in the selection of the working method.

A review of the available data, experience and some classic order of magnitude calculations should lead to the most suitable, digital simulation technique(s). Their application is by no means restricted to large areas. For example boundary conditions, such as streamflow infiltration, interference of wells, effects of impermeable or semipermeable layers or vertical boundaries might be analysed at any scale. Computer models have also made it feasible to analyse groundwater problems simultaneously under transient, non-homogeneous and anisotropic conditions, an achievement unmatched by any other means.

Although the application of proved digital simulation techniques is convenient, cost- and time-saving, other methods should not be neglected in order to reach the objectives for an aquifer evaluation. Any check or reliable interim solution is an asset in the complex field of regional hydrogeology.

2. Remote infrared sensing

2.1. Introduction

Every object having a temperature above absolute zero continously gives off electromagnetic radiation in proportion to its temperature. At higher temperatures a part of the radiation becomes visible as light. At lower temperatures the radiation falls partly into the infrared portion of the spectrum (fig. 8 and 9). Although these radiations are

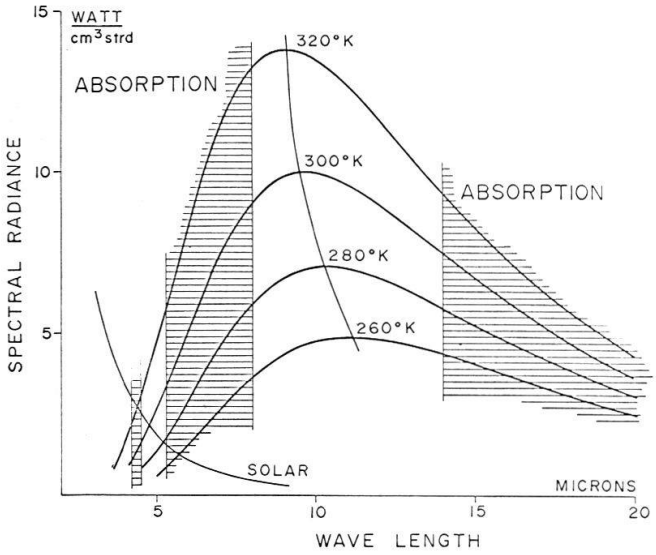

Fig. 8: Absorption effect of the atmosphere: The crosshatched areas show the wave-length that are largely absorbed by carbon dioxide and water vapour in the atmosphere. The unhatched portions represent the co-called «windows» through the atmosphere. There are two main windows in the infrared spectrum, the 3–5 micron and the 8–14 micron (from SLANEY et al.).

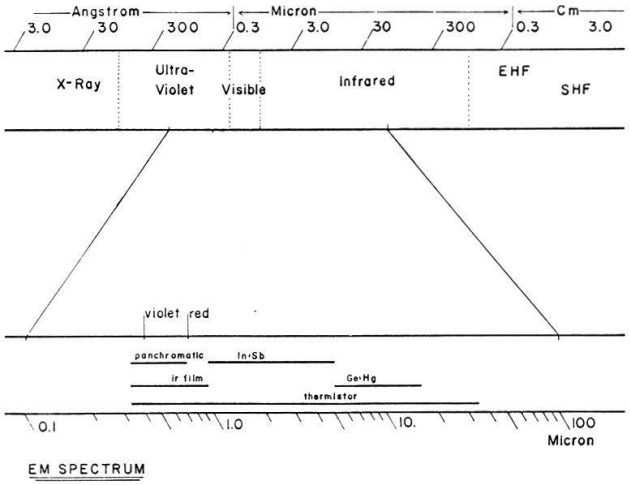

Fig. 9: Part of the electromagnetic spectrum ranging from X-rays through ultra-violet into the visible, the infrared and the microwave bands. The bottom portion of the figure shows an expanded view of the range from upper ultra-violet to the visible and the infrared (from SLANEY et al.).

invisible, they may be detected by a special measuring device. Detection techniques developed in the past years have made it possible to record temperature differences of less than 0.01 °C.

An infrared image is taken from an airecraft in much the same way as a normal aerial photograph (fig. 10). A rotating mirror as scanning device, scans the terrain in continuous strips. The photographic images of thermal sources are abtained indirectly. Infrared photos striking a detector generate an electric signal that varies in intensity according to the amount of thermal energy coming from the part of the terrain viewed by the mirror. The signal is amplified and becomes visible on a glow tube or cathode ray tube which is focused onto a special photographic film. Ordinary film is not sensitive to wavelength in the thermal infrared region. If a black/white IR film is used, warmer temperatures appear as light areas and the cooler temperature as dark areas on the imagery.

2.2. Application

The application of infrared detectors is very versatile. Almost any discipline of the natural sciences might benefit from the remote sensing method. However, since the IR scanner has no penetrating power, it measures and records on film only the radiation from the top few layers of molecules. This peculiarity restricts its application in the field of hydrogeology to special cases, which are nevertheless impressive. The method can

- locate concentrated groundwater outflow into sea, lakes and rivers, which could lead to the exploitation of new groundwater resources;
- locate geothermal springs or geothermal high temperature areas to tap steam for power production;

- expose seepage in- and outlets of dams and reservoirs to locate leakage spots;
- locate new aquifers with high groundwater level, particulary in arid zones;
- identify soil moisture variations and evapotranspiration from groundwater to resolve soil salinity problems.

2.3. Example

An attempt was made to detect concentrated groundwater inflow along the shore by means of temperature surveys in Lake Ontario and by remote infrared scanning from an aircraft. The temperature of groundwater occurring at a depth of 10 to 28 meters generally exceeds the mean annual air temperature by 1 to 2 °C. The annual range of the earth's temperature at this depth may be expected to be less than 1 °C (TODD, 1959). At greater depths the temperature increases approximately 1 °C for each 30 meters. The average annual temperature is approximately 7 °C in the Lake Ontario basin, while the temperature of the groundwater for the upper 30 meters varies from about 8 to 11 °C. In comparison to the upper few meters of the lake water the groundwater is expected to be warmer during the winter months and colder during the summer and early fall.

Accordingly, it should be possible to detect groundwater discharge into the lake, particularly strong local discharges. If the average velocity of the groundwater inflow is less than 1 m/day compared to current velocities of from 0.05 to 0.4 m/sec. (WEILER, 1968) in Lake Ontario, any temperature difference between groundwater infiltrating the lake bottom and the lake water itself could be dissipated very quickly. To make

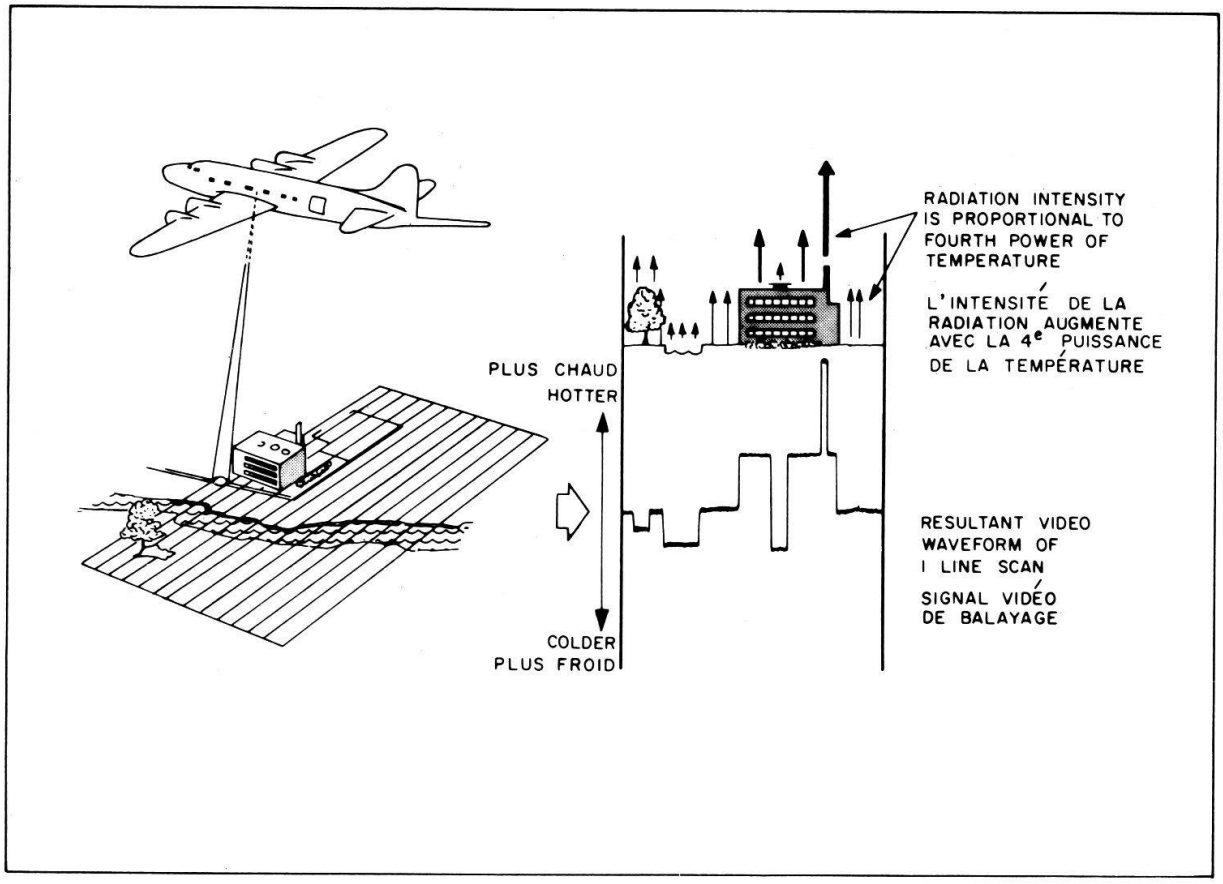

Fig. 10: Left: scanner scans sequential swaths on terrain below the aircraft. Right: a cross section of one such swath. (from DE VILLIERS).

Fig. 11: Infrared images mounted on an aerial photograph of Anaehoomalu Bay (Hawai). The thermal anomaly produced by groundwater outflow is indicated by black arrow (from ADAMS et al.).

detection possible, the velocity of the groundwater presumably has to be very large and its inflow should be concentrated locally. These requirements might be fulfilled by buried valleys containing highly permeable gravel deposits, or by large open bedrock fractures, or extremely high hydraulic gradients in moderately permeable material.

In connection with infrared survey experiments in Canada, H. R. B. Singer Inc. carried out flights in October 1965 along the shore between Cobourg and Niagara-on-the-Lake. For the present study, additional flights over the same area were performed in March 1969 and 1970 by the National Research Council.

The IR imagery is well suited, as SLANEY, GROSS and MORLEY (1969) pointed out, for examining details of the temperature changes in water bodies. The thermal sensitivity of the equipment depends on the temperature range of the scan area on the ground; the smaller the temperature range, the better the accuracy. The smallest temperature change the instrument is capable of detecting is about 0.01 °C. Since most of the time the land surface has a much different temperature than the lake water, the accuracy of the method used at the present time along the shoreline is drastically reduced. This and

the capability of recording only temperatures of the skin of the water appear to be the major shortcomings in the endeavor to pinpoint groundwater outlets. Nevertheless, positive results have been obtained in this field by SLANEY, GROSS and MORLEY (1969) along the Ottawa river (Vaudreuil area), pinpointing groundwater infiltration through buried channels into the river. Another example is the discovery of a groundwater stream flowing into the sea at Anaehoomalu Bay, Hawaii, by ADAMS, PETERSON et al. (fig. 11).

Probably because of the low turbulence in the lake, the best imagery was obtained in October 1965 from an altitude of 1500 m. Aside from three questionable small spots, all anomalies were recorded along high bluffs between Cobourg and Toronto (fig. 12). Unfortunately, the quality of the IR imagery did not allow any interpretation for the area between Hamilton and Niagara-on-the-Lake. The relationship between high steep shores and cold water anomalies, observed also to a minor degree on a boat survey, seemed to be significant. It may be explained in terms of groundwater discharge along the bottom of the bluffs where the hydraulic gradient may be large. The groundwater level in the 4-kilometer wide shorebelt is 3–6 m below the surface and it declines rapidly in the direction of the bluffs, which are up to 80 m high. The hydraulic gradient, and

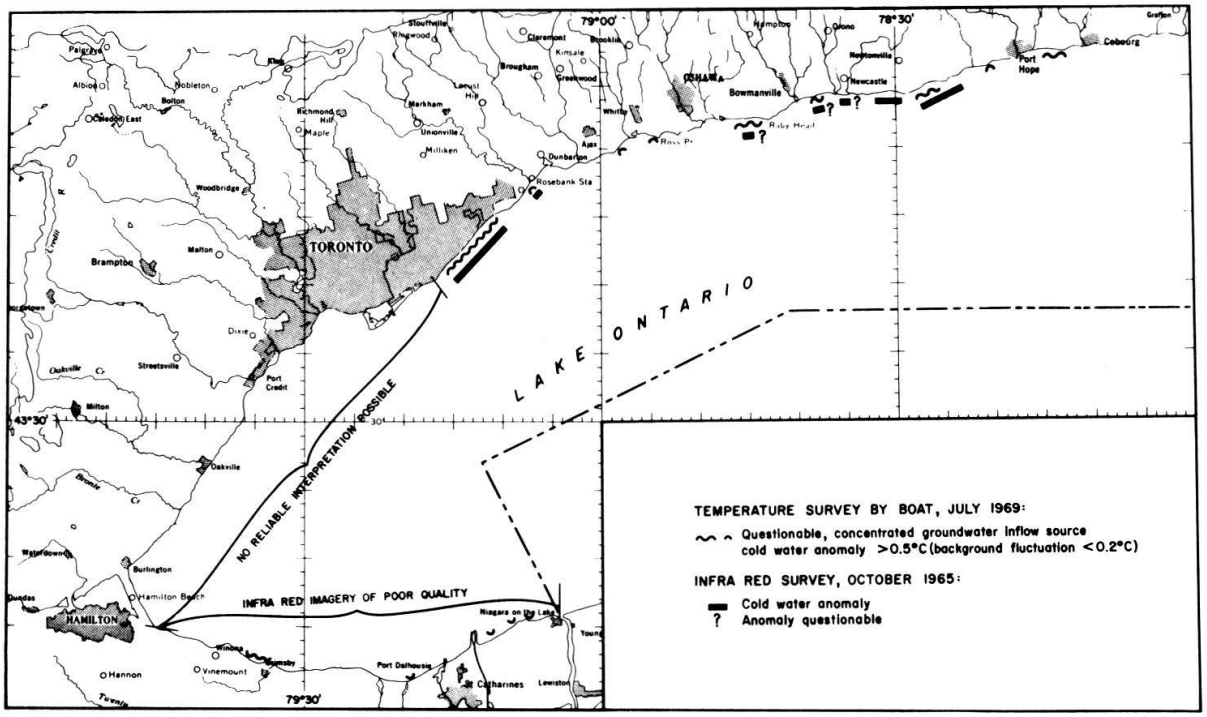

Fig. 12: Locations of concentrated groundwater outflow sources detected by temperature and infrared surveys.

with it the groundwater velocity, may increase in these areas by two orders of magnitude or more, causing a concentrated shallow groundwater outflow close to the lake surface. Figures 13 and 14 show two such temperature anomalies at Scarborough and east of Newcastle between Bouchette Point and Crysler Point.

Althrough infrared surveys were rather limited, substantial anomalies other than those related to the bluffs were not detected. This may be interpreted as indicating the absence of local large groundwater discharge, or it may be taken as an indication that the low temperature effect of groundwater discharge is masked in some areas by other influences such as currents, wind and industrial and municipal waste disposal.

If the facilities are available, and under favorable natural conditions, it is desirable to

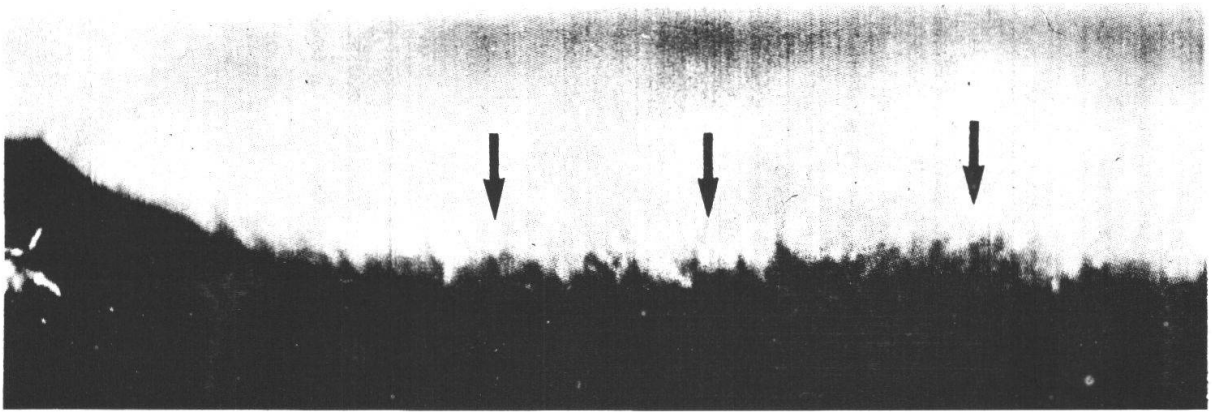

Fig. 13: Infrared imagery at Birch Cliff, Scarborough, outflow is indicated by black arrows (scale approx. 1:43000).

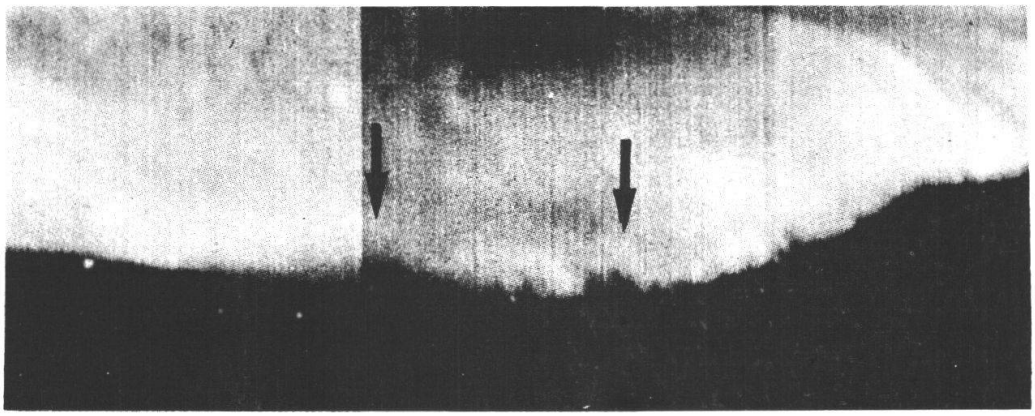

Fig. 14: Infrared imagery between Bouchette Point and Crysler Point, west of Port Hope, outflow indicated by black arrows (scale approx. 1:43000).

verify the result of the remote sensing method by ground controls. In cooperation with the Canada Centre for Inland Waters (CCIW) at Burlington, a temperature survey from a boat was performed in July 1969 along the shore from Niagara-on-the-Lake to Kingston. The launch was instrumented with a single channel recorder, a thermistor bridge with selector switch and three temperature sensors having an accuracy of $\pm 0.1\,^{\circ}C$ and a time constant (response time) of approximately 0.2 second. One sensor was installed at the cooling water intake of the boat motor underneath the hull, approximately 0.3 m below water level; and the third sensor was used to perform vertical profiles. The survey was carried out at an approximate lake depth of 3–4 m with the depth being controlled

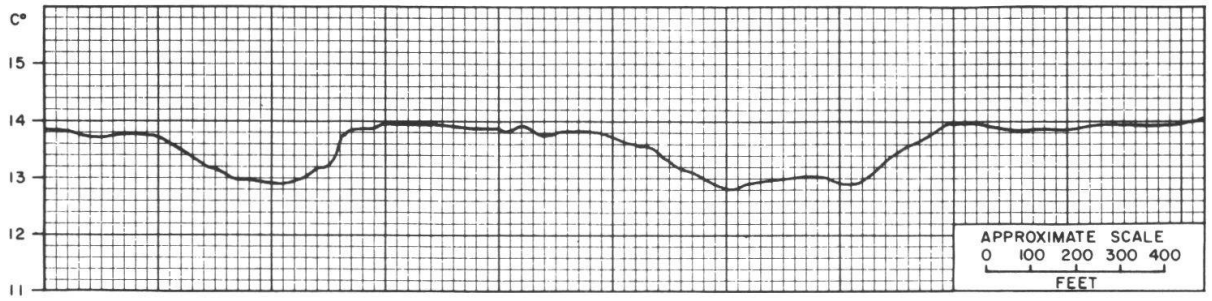

Fig. 15: Chart of temperature survey by boat showing erratic anomalies along cliffs west of Grimsby.

by a recording echo sounder. First, horizontal profiles along the shore were taken at a speed of 8–12 km/hour. Then vertical profiling was attempted at locations where temperature anomalies were indicated. Although the vertical profiling was not completed due to mechanical difficulty, it became apparent that the influence of currents, winds, streams and man made factors (sewage, irrigation, cooling water, etc.) tends to mask effluent groundwater in certain areas. The masking effect appears strongest between Toronto and Hamilton and to a lesser degree between Port Dalhousie and Niagara-on-the-Lake. Cold anomalies for which none of the above mentioned factors could be related are considered to be groundwater inflow spots and are marked as such in Figure 12. Cool anomalies do not appear to correspond to the locations of buried bedrock channels, which generally are filled with rather low permeable till deposits. No remarkable anomalies were found east of Trenton where concentrated inflow through fractures or karstic hollow spaces could occur. However, along steep bluffs, erratic temperature changes were sometimes observed (fig. 15), confirming the results of the infrared survey.

Selected References

Adams, W. A., F. L. Peterson, S. P. Mathur, L. K. Lepley, C. Warren and R. D. Huber (1971): A hydrogeophysical survey using remote-sensing methods from Kawaihae to Kailua-Kona, Hawaii. Groundwater, Jan.–Feb. 1971, Vol. 9, No. 1.

California, State of (1966): Planned utilisation of groundwater basins, San Gabriel Valley. Department of Water Resources, Bull. No. 104/2, March 1966.

Freeze R. A., and P. A. Witherspoon (1966): Theoretical analysis of regional groundwater flow – I. analytical and numerical solutions to the mathematical model. Water Resources Research, Vol. 2, No. 4.

Haefeli, C. J. (1972): Groundwater inflow into Lake Ontario from the Canadian side. Inland Water Branch, Department of the Environment, Scientific Series No. 9.

Pinder, G. F., and J. D. Bredehoft (1968): Application of the digital computer for aquifer evaluation. Water Resources Research, Vol. 4, No. 5.

Slaney, V. R., H. Gross and L. W. Morley (1969): Airborne infrared scanning survey along the shorelines of the lower Great Lakes. Department of Energy, Mines and Resources, Publication of the Geological Survey of Canada.

Todd, D. K. (1959): Groundwater Hydrology. John Wiley and Sons Inc. London and Sidney.

de Villiers, N. (1969): Develop infrared scanner for Canadian uses. Science Dimension, National Resources Council of Canada, Vol. 1, No. 1, June 1969.

Weiler, H. S. (1968): Current measurements in Lake Ontario in 1967. Department of Energy, Mines and Resources, Inland Water Branch, Reprint Series No. 46.